Photosynth Res (2014) 121:265–275
DOI 10.1007/s11120-014-9984-9

REGULAR PAPER

Strong shift from HCO_3^- to CO_2 uptake in *Emiliania huxleyi* with acidification: new approach unravels acclimation versus short-term pH effects

Dorothee M. Kottmeier · Sebastian D. Rokitta · Philippe D. Tortell · Björn Rost

Received: 7 October 2013 / Accepted: 10 February 2014 / Published online: 23 February 2014

Abstract Effects of ocean acidification on *Emiliania huxleyi* strain RCC 1216 (calcifying, diploid life-cycle stage) and RCC 1217 (non-calcifying, haploid life-cycle stage) were investigated by measuring growth, elemental composition, and production rates under different pCO_2 levels (380 and 950 µatm). In these differently acclimated cells, the photosynthetic carbon source was assessed by a ^{14}C disequilibrium assay, conducted over a range of ecologically relevant pH values (7.9–8.7). In agreement with previous studies, we observed decreased calcification and stimulated biomass production in diploid cells under high pCO_2, but no CO_2-dependent changes in biomass production for haploid cells. In both life-cycle stages, the relative contributions of CO_2 and HCO_3^- uptake depended strongly on the assay pH. At pH values $\leq$ 8.1, cells preferentially used CO_2 ($\geq$ 90 % CO_2), whereas at pH values $\geq$ 8.3, cells progressively increased the fraction of HCO_3^- uptake ($\sim$45 % CO_2 at pH 8.7 in diploid cells; $\sim$55 % CO_2 at pH 8.5 in haploid cells). In contrast to the short-term effect of the assay pH, the pCO_2 acclimation history had no significant effect on the carbon uptake behavior. A numerical sensitivity study confirmed that the pH-modification in the ^{14}C disequilibrium method yields reliable results, provided that model parameters (e.g., pH, temperature) are kept within typical measurement uncertainties. Our results demonstrate a high plasticity of *E. huxleyi* to rapidly adjust carbon acquisition to the external carbon supply and/or pH, and provide an explanation for the paradoxical observation of high CO_2 sensitivity despite the apparently high HCO_3^- usage seen in previous studies.

Keywords CO_2 concentrating mechanism · pH · Inorganic carbon source · Coccolithophore · Ocean acidification · Isotopic disequilibrium · Photosynthesis

Introduction

Marine phytoplankton account for $\sim$50 % of global primary production and are the main drivers of the marine "particulate organic carbon" (POC) pump (Falkowski et al. 1998; Field et al. 1998). Calcifying phytoplankton species also contribute to the "particulate inorganic carbon" (PIC) pump and thereby play a dual role in regulating marine biogeochemical cycling of carbon through their effects on surface ocean alkalinity (Broecker and Peng 1982; Zeebe and Wolf-Gladrow 2007). One key species of calcifying phytoplankton is the cosmopolitan and bloom-forming coccolithophore *Emiliania huxleyi*, which has been established as a model organism over the recent decades (Paasche 2002; Raven and Crawfurd 2012; Read et al. 2013; Westbroek et al. 1993). While the calcifying diploid life-cycle stage of this species has been intensively studied in field and laboratory experiments, the non-calcifying haploid stage has only recently gained attention due to its important ecological role. In blooms of diploid *E. huxleyi*, which are usually terminated by viruses, the haploid life-

Electronic supplementary material The online version of this article (doi:10.1007/s11120-014-9984-9) contains supplementary material, which is available to authorized users.

Guest Editor: James Moroney.

D. M. Kottmeier (✉) · S. D. Rokitta · B. Rost
Alfred Wegener Institute Helmholtz Centre for Polar and Marine Research, Am Handelshafen 12, 27570 Bremerhaven, Germany
e-mail: Dorothee.Kottmeier@awi.de

P. D. Tortell
Department of Earth Ocean and Atmospheric Sciences, and Deparment of Botany, University of British Columbia, Vancouver, BC V6TZ4, Canada

cycle stage functions as a virus-resistant backup population (Frada et al. 2012). Furthermore, the presence and absence of calcification in the differing life-cycle stages of *E. huxleyi* make them ideal candidates to investigate the cellular mechanisms of calcification and their interaction with photosynthesis under increasing oceanic CO_2 concentrations (Mackinder et al. 2010; Rokitta and Rost 2012).

Increasing pCO_2 in oceanic surface water directly affects carbonate chemistry by elevating the concentration of dissolved inorganic carbon (DIC) and shifting the carbon speciation toward higher CO_2 and H^+ concentrations, a phenomenon often referred to as ocean acidification (OA; Caldeira and Wickett 2003; Wolf-Gladrow et al. 1999). Compared to preindustrial values, pH is expected to drop by 0.4–0.5 units until the end of this century. In several studies testing the effects of OA on *E. huxleyi*, diploid strains were found to exhibit strong, yet opposing responses in terms of biomass and calcite production. While biomass production was either unaffected or stimulated by increased pCO_2, calcification typically decreased and malformations of coccoliths increased (e.g., Hoppe et al. 2011; Langer et al. 2009; Riebesell et al. 2000). Bach et al. (2011) suggested that biomass production is stimulated by increasing CO_2 concentration at sub-saturating conditions, whereas calcification is specifically responsive to the associated decrease in pH. Such differential CO_2 and pH effects on biomass and calcite production are supported by the observation that OA distorts ion homeostasis and shifts the metabolism from oxidative to reductive pathways (Rokitta et al. 2012; Taylor et al. 2011). In a number of studies, the sensitivity of *E. huxleyi* toward OA has been attributed to its mode of inorganic carbon (C_i) acquisition, which is intrinsically responsive to changes in carbonate chemistry. Thus, for understanding the differential responses to OA, one needs to look at this crucial process of C_i assimilation.

Like most phytoplankton, *E. huxleyi* operates a CO_2 concentrating mechanism (CCM), which utilizes CO_2 and/or HCO_3^- uptake systems to accumulate CO_2 in the vicinity of RubisCO, and employs the enzyme carbonic anhydrase (CA) to accelerate the inter-conversion between these C_i species (see Reinfelder 2011 for review). For a long time, the CCM in *E. huxleyi* was assumed to rely on the CO_2 delivery by calcification (Anning et al. 1996; Sikes et al. 1980). More recently, however, studies have demonstrated that C_i fluxes for photosynthesis and calcification are independent (Herfort et al. 2004; Rost et al. 2002; Trimborn et al. 2007), and that these two processes may even compete for C_i substrates (Rokitta and Rost 2012). Most studies performed on the CCM of *E. huxleyi* to date yielded moderately high substrate affinities for C_i, which decreased slightly under OA scenarios (e.g., Rokitta and Rost 2012; Rost et al. 2003, Stojkovic et al. 2013). Moreover, low activity for extracellular CA and high contribution of HCO_3^- uptake for photosynthesis have been reported (e.g., Herfort et al. 2002; Rokitta and Rost 2012; Stojkovic et al. 2013; Trimborn et al. 2007). This high apparent HCO_3^- usage is puzzling, however, as it suggests biomass production to be rather insensitive to OA-related changes in CO_2 supply, which is in contrast to what studies usually have observed.

Most physiological methods characterizing the CCM and its functional elements are performed under standardized assay conditions, including a fixed pH value, and thus differing from treatment conditions. The pH and the concominant C_i speciation can, however, influence the cell's physiology, in particular its C_i acquisition. When identifying the cause-effect relationship in OA responses, it is difficult to separate the effects of changes in C_i speciation from concomitant changes in H^+ concentrations. Changes in external pH have been shown to directly drive changes in cytosolic pH in *E. huxleyi*, which, in turn, affected H^+ gradients and membrane potentials (Suffrian et al. 2011; Taylor et al. 2011). This effect could indirectly impact secondary active transporters, e.g., the Cl^-/HCO_3^- antiporter (Herfort et al. 2002; Rokitta et al. 2011). Moreover, the protonation of amino acid side chains can affect activity, specificity, and kinetics of enzymes and transporters involved in cellular processes (Badger 2003; Raven 2006). Hence, aside from altered concentrations of C_i species, pH itself could directly impact the mode of CCM (Raven 1990). These possible effects of the assay pH on C_i acquisition should be accounted for when performing experiments to characterize the CCM.

One common approach to determine the C_i source for photosynthesis is the application of the ^{14}C disequilibrium method (Espie and Colman 1986), which has proven suitable for the study of marine phytoplankton in laboratory cultures (e.g., Elzenga et al. 2000; Rost et al. 2006a) and in natural field assemblages (e.g., Cassar et al. 2004; Martin and Tortell 2006; Tortell and Morel 2002; Tortell et al. 2008). The method makes use of the relatively slow chemical conversion between the CO_2 and HCO_3^- in the absence of CA (Johnson 1982), allowing for a differential labeling of these C_i species with ^{14}C. This method is typically performed at pH of 8.5 ("assay pH"), deviating strongly from most natural in situ values and even more from the pH values applied in OA-experiments ("acclimation pH"). In this study, we aimed to disentangle the short-term effect of assay pH from the long-term effect of acclimation history on the photosynthetic C_i source of *E. huxleyi*. To this end, we grew haploid and diploid life-cycle stages at present-day (380 µatm) and elevated pCO_2 (950 µatm), and measured the responses in growth, elemental composition, and production rates. These low and high pCO_2-acclimated cells were then tested for their preferred C_i source by applying the ^{14}C disequilibrium

method, with assay conditions set to a range of ecologically relevant pH values (pH 7.9–8.7). The reliability of this new approach was tested by performing sensitivity studies.

Methods

pCO_2 acclimations

Haploid and diploid cells of *E. huxleyi* (strains RCC 1217 and RCC 1216, obtained from the Roscoff culture collection) were grown at 15 °C as dilute batch incubations. North Sea seawater medium (salinity 32.4) was sterile-filtered (0.2 µm) and enriched with vitamins and trace metals according to F/2 (Guillard and Ryther 1962), as well as phosphate and nitrate (100 and 6.25 µmol L^{-1}). Cells were exposed to a light:dark cycle (16:8 h) and saturating light (300 µmol photons m^{-2} s^{-1}) provided by daylight lamps (FQ 54W/965HO, OSRAM, Munich, Germany). Light intensity was monitored with the LI-6252 datalogger (LI-COR, Lincoln, NE, USA) using a 4π-sensor (US-SQS/L, Walz, Effeltrich, Germany). Culturing was carried out in sterilized 2.4 L borosilicate bottles (Duran Group, Mainz, Germany) on roller tables to avoid sedimentation.

Prior to experiments, cells were acclimated to the respective pCO_2 and light conditions for at least 7 days (i.e., more than 10 generations). Prior to initiating cultures, medium was pre-aerated for at least 36 h with humidified, 0.2 µm-filtered air comprising pCO_2 values of 380 or 950 µatm (equivalent to 38.5 and 96.3 Pa, or ~15 and ~35 µmol kg^{-1}, respectively). Gas mixtures were created by a gas flow controller (CGM 2000 MCZ Umwelttechnik, Bad Nauheim, Germany) using pure CO_2 (Air Liquide Deutschland, Düsseldorf, Germany) and CO_2-free air (CO2RP280, Dominick Hunter, Willich, Germany). Sampling and measurements were done 4–8 h after the beginning of the light period (i.e., at midday) in exponential growth at densities of 40,000–60,000 cells mL^{-1}. Cultures showing a pH drift of > 0.05 were excluded from further analyses.

The carbonate system (Table 1) during the acclimations was assessed based on measurements of pH and total alkalinity (TA). The pH_{NBS} of the cultures was measured potentiometrically and corrected for temperature (pH-meter 3110; WTW, Weilheim, Germany). The electrode (A157, Schott Instruments, Mainz, Germany) was three-point calibrated with NBS certified standard buffers and the measurement uncertainty was 0.03 pH units. TA was determined by potentiometric titration (Dickson 1981; TitroLine alpha plus, Schott Instruments). Measurements were accuracy-corrected with certified reference materials (CRMs) supplied by A. Dickson (Scripps Institution of Oceanography, USA). Calculation of the carbonate system was performed using CO2sys (Pierrot et al. 2006). Input parameters were pH_{NBS} and TA, as well as temperature (15 °C), salinity (32.4), and pressure (1 dbar, according to 1 m depth; Hoppe et al. 2012). For all calculations, phosphate and silicate concentrations were assumed to be 7 and 17 µmol kg^{-1}, respectively, based on assessments of the media. Equilibrium constants for carbonic acid, K_1 and K_2 given by Mehrbach et al. (1973) and refit by Dickson and Millero (1987) were used. For the dissociation of sulfuric acid, the constants reported by Dickson (1990) were employed.

Cell growth was assessed by daily cell counting with a Multisizer III hemocytometer (Beckman-Coulter, Fullerton, CA, USA) and the specific growth rates (μ) were calculated from daily increments (cf., Rokitta and Rost 2012). For the determination of total particulate carbon (TPC), POC and particulate organic nitrogen (PON), cell suspensions were vacuum-filtered (-200 mbar relative to atmosphere) onto pre-combusted (12 h, 500 °C) GF/F filters (1.2 µm; Whatman, Maidstone, UK), which were dried at 65 °C and analyzed with a EuroVector CHNS-O elemental analyzer (EuroEA, Milano, Italy). Before quantification of POC, filters were HCl-soaked (200 µL, 0.2 M) and dried to remove calcite. PIC was assessed as the difference between TPC and POC. By multiplying the POC and PIC cell quotas with μ, the respective production rates were derived (cf., Rokitta and Rost 2012). For Chl *a* measurements, cells were filtered onto cellulose nitrate filters (0.45 µm; Sartorius, Göttingen, Germany) and instantly frozen in liquid nitrogen. Chl *a* was extracted in 90 % acetone (v/v, Sigma, Munich, Germany) and determined fluorometrically (TD-700 fluorometer, Turner Designs, Sunnyvale, USA) following the protocol by Holm-Hansen and Riemann (1978). The calibration of the fluorometer was carried out with a commercially available Chl *a* standard (*Anacystis nidulans*, Sigma, Steinheim, Germany).

^{14}C disequilibrium method

The C_i source for photosynthesis was determined by applying the ^{14}C disequilibrium method (Elzenga et al. 2000; Espie and Colman 1986; Tortell and Morel 2002). In this method, a transient isotopic disequilibrium is induced by adding a small volume of a $^{14}C_i$ "spike" solution with a relatively low pH (typically 7.0) into larger volume of buffered cell suspension with a relatively high pH (typically 8.5). The cell suspension contains dextran-bound sulfonamide (DBS) to eliminate possible external CA activity. Due to the pH-dependent speciation of DIC, the relative CO_2 concentration of the spike is high (~19 % of DIC at pH 7.0), compared to the cell suspension (~0.3 % of DIC at pH 8.5). When adding the spike to the cell suspension, the majority of the CO_2 added with the spike

Table 1 Carbonate chemistry of the pCO_2 acclimations at the time of harvesting and in cell-free media (reference); Attained pCO_2, DIC, HCO_3^-, CO_3^{2-}, and $\Omega_{calcite}$ are calculated based on measured pH_{NBS} and TA using CO2sys (Pierrot et al. 2006)

Strain, ploidy	Treatment pCO_2 (µatm)	Attained pCO_2 (µatm)	pH_{NBS}	TA (µmol kg^{-1})	DIC (µmol kg^{-1})	CO_2 (µmol kg^{-1})	HCO_3^- (µmol kg^{-1})	CO_3^{2-} (µmol kg^{-1})	$\Omega_{calcite}$
RCC 1216, 2N	Low, 380	353 ± 8	8.19 ± 0.02	2,259 ± 19	2,023 ± 15	13 ± 0	1,857 ± 13	161 ± 3	3.9 ± 0.1
	High, 950	847 ± 55	7.86 ± 0.04	2,278 ± 20	2,156 ± 2	32 ± 2	2,060 ± 28	84 ± 4	2.0 ± 0.1
RCC 1217, 1N	Low, 380	345 ± 4	8.23 ± 0.00	2,317 ± 12	2,068 ± 10	13 ± 0	1,885 ± 10	170 ± 1	4.1 ± 0.0
	High, 950	837 ± 25	7.89 ± 0.01	2,317 ± 3	2,210 ± 5	32 ± 1	2,092 ± 5	86 ± 3	2.1 ± 0.1
Cell-free medium	Low, 380	405 ± 3	8.17 ± 0.00	2,304 ± 5	2,092 ± 5	15 ± 0	1,926 ± 5	151 ± 1	3.7 ± 0.0
	High, 950	997 ± 17	7.82 ± 0.01	2,305 ± 7	2,214 ± 12	38 ± 1	2,128 ± 11	75 ± 1	1.8 ± 0.0

Results are reported for 15 °C ($n \geq 3$; ± SD)

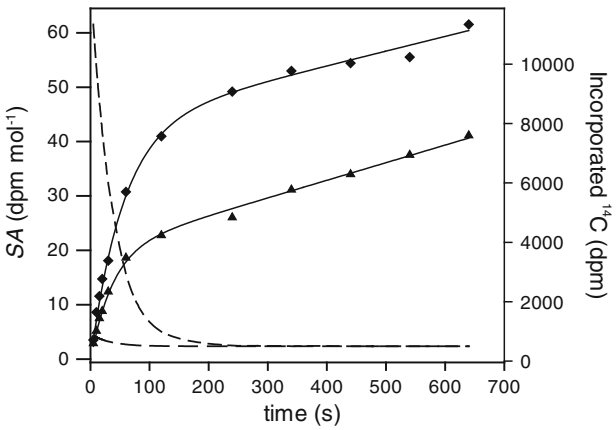

Fig. 1 Time-course of specific activities of CO_2 and HCO_3^- (medium and long dashed lines, respectively, here calculated for assay pH 8.5) in the isotopic disequilibrium method and examples for the ^{14}C incorporation of the diploid life-cycle stage for predominant CO_2 usage ($f_{CO_2} = 1.00$, *squares*) and considerable HCO_3^- usage ($f_{CO_2} = 0.60$, *triangles*)

converts into HCO_3^- until equilibrium is achieved (Johnson 1982; Millero and Roy 1997). Consequently, the specific activity of CO_2 (SA_{CO_2}, dpm (mol CO_2)$^{-1}$) is initially high and exponentially decays over time (Fig. 1). The slope of the ^{14}C incorporation curve of a "CO_2 user" is, therefore, initially much steeper than during final linear ^{14}C uptake, when isotopic equilibrium is achieved. In contrast, the slope of ^{14}C incorporation for "HCO_3^- users" changes only marginally over time because $SA_{HCO_3^-}$ stays more or less constant during the assay.

Quantification of the relative proportion of CO_2 or HCO_3^- usage was done by fitting data with the integral function of the ^{14}C fixation rate (Elzenga et al. 2000; Espie and Colman 1986; Martin and Tortell 2006). The function includes terms representing the instantaneous fixation rate of $DI^{14}C$, the fractional contribution of CO_2 (f_{CO_2}) or HCO_3^- usage ($1 - f_{CO_2}$) to the overall C_i fixation and the specific activity (SA, dpm mol^{-1}) of these substrates at any given time (Eq. 1; Espie and Colman 1986; Elzenga et al. 2000; Tortell and Morel 2002). Strictly speaking, as HCO_3^- and CO_3^{2-} cannot be differentially labeled, $1 - f_{CO_2}$ also comprises the potential fraction of CO_3^{2-} used.

$$\begin{aligned} \text{dpm} = & V_{DI14C}(f_{CO_2})(\alpha_1 t + (\Delta SA_{CO_2}/SA_{DIC})(1 - e^{-\alpha_1 t}))/\alpha_1 \\ & + V_{DI14C}(1 - f_{CO_2})(\alpha_2 t + (\Delta SA_{HCO_3}/SA_{DIC})(1 - e^{-\alpha_2 t}))/\alpha_2 \end{aligned} \quad (1)$$

In this equation, V_{DI14C} is the total rate of ^{14}C uptake; f_{CO_2} is the fraction of uptake attributable to CO_2; α_1 and α_2 are the temperature-, salinity-, and pH-dependent first-order rate constants for CO_2 and HCO_3^- hydration and dehydration, respectively; t is the time (s); ΔSA_{CO_2} and ΔSA_{HCO_3} are the differences between the initial and equilibrium values of the specific activities of CO_2 and HCO_3^-, respectively; and SA_{DIC} is the specific activity of DIC. During steady-state photosynthesis, V_{DI14C} and f_{CO_2} are assumed to be constant so that changes in the instantaneous ^{14}C uptake rate reflect only changes in the specific activity of CO_2 and HCO_3^-.

In the present study, the ^{14}C disequilibrium method was modified to enable measurements over a range of ecologically relevant pH values (7.90–8.70). In order to maintain a suitably large initial isotopic disequilibrium ($\Delta SA_{CO_2}/SA_{DIC}$), the pH of the ^{14}C spike solutions needs to be adjusted in conjunction with the pH of the assay buffer. We, thus, used either MES or HEPES buffers to set the pH of spike solutions over the range of 5.75–7.30 (see Table 2 for exact pH values of assay and spike buffers). For the assays, 10–30 × 10^6 cells were concentrated via gentle filtration over a polycarbonate filter (2 µm; Millipore, Billerica, MA, USA) to a final volume of 15 mL. During this filtration procedure, cells were kept in suspension, while the medium was gradually exchanged with buffered assay medium of the appropriate pH value. Assay media and spike buffers were prepared at least 1 day prior

Table 2 Chemical characteristics of ^{14}C disequilibrium assay media and spike buffers, and the associated parameter values for model fits (Eq. 1)

Assay medium			Spike solution			Conditions for RCC 1216, 2N					Conditions for RCC 1217, 1N				
pH	Buffer chemical	CO_2 (%)	pH	Buffer chemical	CO_2 (%)	DIC (μM)	CO_2 (μM)	α_1	α_2	$\frac{\Delta SA_{CO_2}}{SA_{DIC}}$	$\frac{\Delta SA_{HCO_3^-}}{SA_{DIC}}$	DIC (μM)	CO_2 (μM)	α_1	α_2	$\frac{\Delta SA_{CO_2}}{SA_{DIC}}$	$\frac{\Delta SA_{HCO_3^-}}{SA_{DIC}}$
7.90	BICINE	1.1	5.75	MES	80.4	2,210	23.4	0.0186	0.0197	29.09	−0.786	2,490	26.7	0.0176	0.0186	28.44	−0.786
8.10	BICINE	0.7	6.35	MES	50.7	2,250	14.6	0.0205	0.0225	30.08	−0.451	2,680	17.6	0.0194	0.0212	30.09	−0.454
8.30	BICINE	0.4	6.70	MES	31.5	2,290	8.9	0.0236	0.0272	30.46	−0.204	2,590	10.3	0.0223	0.0256	29.83	−0.206
8.50	BICINE	0.2	7.00	HEPES	18.7	2,380	5.4	0.0285	0.0355	31.37	−0.012	2,310	5.4	0.0270	0.0334	27.87	0.008
8.70	BICINE	0.1	7.30	HEPES	10.3	2,150	2.8	0.0364	0.0504	29.16	−0.237	–	–	–	–	–	–

Assays with the diploid cells (2N) were conducted at an assay temperature of 15.5 °C, a spike temperature of 23 °C, an added radioactivity of 315 kBq and a salinity of 32.4. Assays with the haploid cells (1N) were conducted at an assay temperature of 15.0 °C, a spike temperature of 23 °C, a spike radioactivity of 370 kBq and a salinity of 32.4

to the assay and stored in closed containers to avoid CO_2 exchange and pH drift. The pH value and temperatures of all buffers were measured immediately prior to assay runs. DIC concentration of the assay buffers was determined colorimetrically according to Stoll et al. (2001) using a TRAACS CS800 autoanalyzer (Seal Analytical, Norderstedt, Germany), and measurements were accuracy-corrected with CRMs supplied by A. Dickson (Scripps Institution of Oceanography, USA).

To initiate the assays, a volume of 4 mL buffered concentrated cell suspension was transferred into a temperature-controlled, illuminated glass cuvette (15 °C; 300 μmol photons m^{-2} s^{-1}) to which 50 μM DBS was added (Ramidus, Lund, Sweden). Cells were continuously stirred in the light for at least 5 min prior to spike addition to reach steady-state photosynthesis. Spike solutions were prepared by adding $NaH^{14}CO_3$ solution (1.88 GBq (mmol DIC)$^{-1}$; GE Healthcare, Amersham, UK) into a final volume of 200 μL of pH-buffered MilliQ water (various buffers at 20 mM; Table 2), yielding activities of ~370 kBq (10 μCi). Following the spike addition, 200 μL subsamples of the cell suspension were transferred into 2 mL HCl (6 M) at time points between 5 s and 12 min. Addition of these aliquots to the strong acid caused instant cell death and converted all DIC and PIC to CO_2. $DI^{14}C$ background was degassed in a custom-built desiccator for several days until samples were dry. Deionized water (1 mL) was then added to re-suspend samples prior to addition of 10 mL of scintillation cocktail (Ultima Gold AB, GMI, Ramsey, MN, USA), and the sample was vortexed thoroughly.

Acid-stable (i.e., organic) ^{14}C activity in samples was counted with a Packard Tri-Carb Liquid Scintillation Counter (GMI). Blank samples, consisting of cell-free medium, were treated alongside the other samples. In the few cases where no blanks were available, time zero values were approximated by extrapolating the y-axis intercept from linear fitting of the first three data points of the ^{14}C incorporation curves. Total radioactivity of the $NaH^{14}CO_3$ stock solution was regularly quantified and compared to expected values to estimate loss of radioactivity or changes in counting efficiency. In all spike solutions, measured radioactivity ranged between 80 and 100 % of the theoretical values, and the actual radioactivity levels were used in the calculation of the specific activities. Blank-corrected data were fitted (Eq. 1), using a least-squares-fitting procedure. Applied fit parameters are given in Table 2. Furthermore, a detailed Excel spread sheet for calculating the fit parameters in dependence of the applied conditions (e.g., pH, temperature and DIC concentrations) is provided as Supplementary Material. Please note that in the calculation of initial and final specific activities, we accounted not only for changes in concentrations of $^{14}C_i$ species but also for

Table 3 Growth rates, elemental quotas and production rates, elemental ratios, as well as pigment composition of haploid (1N) and diploid (2N) cells of *E. huxleyi*, cultured at low (380 µatm) and elevated pCO_2 (950 µatm): μ (day^{-1}), POC quota (pg $cell^{-1}$), POC production (pg $cell^{-1}$ day^{-1}), PIC quota (pg $cell^{-1}$), PIC production (pg $cell^{-1}$ day^{-1}), TPC quota (pg $cell^{-1}$), TPC production (pg $cell^{-1}$ day^{-1}), PON quota (pg $cell^{-1}$), PON production (pg $cell^{-1}$ day^{-1}), PIC:POC ratio (mol:mol), POC:PON ratio (mol:mol), Chl *a* quotas (pg $cell^{-1}$), and Chl *a*:POC ratios (pg:pg)

Parameter	1N low pCO_2	1 N high pCO_2	p	2N low pCO_2	2N high pCO_2	p
μ	1.12 ± 0.04	1.08 ± 0.06	†	1.08 ± 0.05	1.04 ± 0.04	†
POC quota	10.76 ± 0.23	11.08 ± 1.19	†	8.35 ± 0.84	14.78 ± 1.91	**
POC production	12.09 ± 0.25	12.81 ± 0.44	†	9.02 ± 0.91	13.97 ± 0.63	*
PIC quota	0.48 ± 0.43	−0.18 ± 0.21	†	11.78 ± 0.78	10.90 ± 0.60	†
PIC production	–	–	†	12.71 ± 0.29	11.35 ± 0.90	**
TPC quota	11.23 ± 0.66	12.01 ± 1.27	†	20.13 ± 1.34	25.68 ± 2.00	*
TPC production	12.63 ± 0.70	12.51 ± 0.52	†	21.73 ± 1.05	26.77 ± 3.10	≤ 0.06
PON quota	1.39 ± 0.06	1.45 ± 0.09	†	1.54 ± 0.12	1.95 ± 0.22	*
PON production	1.56 ± 0.06	1.56 ± 0.08	†	1.66 ± 0.10	2.03 ± 0.30	†
PIC:POC	–	–	†	1.42 ± 0.14	0.75 ± 0.11	**
POC:PON	9.03 ± 0.19	8.90 ± 0.69	†	6.31 ± 0.30	8.83 ± 0.17	***
Chl *a* quota	0.10 ± 0.01	0.12 ± 0.01	†	0.18 ± 0.01	0.17 ± 0.01	†
Chl *a* :POC	0.009 ± 0.001	0.012 ± 0.001	†	0.022 ± 0.001	0.012 ± 0.001	***

For the haploid cells, PIC production and PIC:POC ratios were not calculated. Stars indicate statistical significance levels in differences between low and high pCO_2 treatments with * $p \leq 0.05$, ** $p \leq 0.01$ and *** $p \leq 0.001$. No significant difference ($p > 0.05$) is indicated by †

changes in concentrations of $DI^{12}C$, $^{12}CO_2$, and $H^{12}CO_3^-$ upon spike addition. If these changes are neglected, $\Delta SA_{CO_2}/SA_{DIC}$ will be significantly overestimated, leading to an underestimation of f_{CO_2} (Eq. 1, Table 2, Supplementary material).

We used a numerical sensitivity study to examine how offsets in parameters such as pH, DIC concentrations, radioactivity, temperature, or blank values influence the derived estimates of f_{CO_2}. First, theoretical ^{14}C incorporation curves for "HCO_3^- users" ($f_{CO_2} = 0.25$) and "CO_2 users" ($f_{CO_2} = 0.80$) were generated for two assay pH values (7.90 and 8.50) and used as a reference, assuming fixed values of DIC concentrations of 2,300 µmol kg^{-1}, assay temperature of 15 °C, spike solution temperature of 23 °C and spike radioactivity of 370 kBq. In a second step, model fits were obtained using slight offsets in these parameters (e.g., pH 7.95 and 7.85 instead of 7.90) to obtain the effect of parameter variability on f_{CO_2} estimates. Sensitivity toward over- and underestimation of pH, temperature, DIC concentration, and radioactivity was tested. We further assessed the effects of blank values (±100 dpm) on f_{CO_2} estimates as a function of different final ^{14}C incorporation rates.

Statistics

All experiments were performed using at least biological triplicates (i.e., three independent, but equally treated cultures). When data were normally distributed (Shapiro-Wilk test) and showed equal variance (Equal-Variance Test), significance in difference between pCO_2 treatments was tested by performing student's t-tests. When samples were not normally distributed or did not show equal variance, a rank sum test was performed instead. Null hypotheses were rejected when $p \leq 0.05$, unless otherwise indicated.

Results

In diploid cells of *E. huxleyi*, the specific growth rate μ and PIC quotas did not change significantly in response to elevated pCO_2 (Table 3). While there was a small decrease in PIC production rates (−11 %), POC quotas and production rates increased strongly under elevated pCO_2 (+77 and +55 %, respectively). In conjunction with these changes, the quotas and production rates of TPC also increased (+28 and +23 %, respectively). The PIC:POC ratios of diploid cells decreased from 1.4 to 0.7 under elevated pCO_2, while the POC:PON ratios increased from 6.3 to 8.8. Chl *a* quotas were largely unaffected by the pCO_2 treatments, although Chl *a*:POC ratios decreased significantly from 0.022 to 0.012 pg pg^{-1} under elevated pCO_2, owing to the change in POC quotas. In haploid cells, neither μ, elemental quotas or the respective production rates showed any significant response to elevated pCO_2

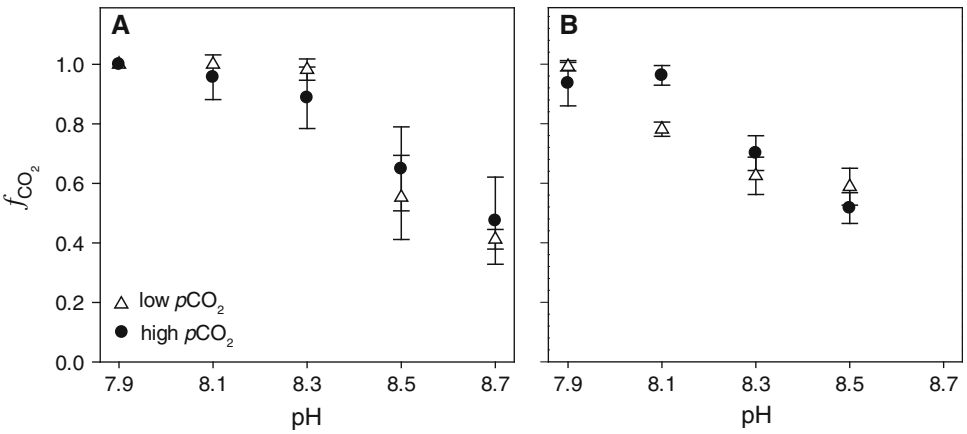

Fig. 2 Fraction of CO_2 usage (f_{CO_2}) as a function of the assay pH in **A** the diploid *E. huxleyi* RCC 1216 and **B** the haploid RCC 1217 being acclimated to low pCO_2 (380 µatm, *white triangles*) and high pCO_2 (950 µatm, *black circles*)

(Table 3). Similarly, Chl *a* quotas, Chl *a*:POC, and POC:PON ratios were all unaffected by the experimental CO_2 manipulations in the haploid strain.

Under both pCO_2 acclimations, diploid cells were shown to be predominant "CO_2 users" under low assay pH ($f_{CO_2} \sim 1.0$ at pH 7.9; Fig. 2a). With increasing assay pH, however, we observed a significant increase in relative HCO_3^- utilization. HCO_3^- uptake was induced at assay pH $\geq$ 8.3 (equivalent to CO_2 concentrations $\leq$ 9 µmol L^{-1}), reaching considerable contribution at high assay pH ($f_{CO_2} \sim 0.44$ at pH 8.7). In contrast to the strong effect of the assay pH, the tested pCO_2 acclimations had no effect on the pH-dependent C_i uptake behavior (Fig. 2a). In other words, both low and high pCO_2-acclimated cells showed the same short-term response of f_{CO_2} to assay pH. Like the diploid stage, haploid cells progressively changed from high CO_2 usage at low assay pH ($f_{CO_2} \sim 0.96$ at pH 7.9) to substantial HCO_3^- contributions when assays were conducted in high pH assay buffers ($f_{CO_2} \sim 0.55$ at pH 8.5; Fig. 2b). HCO_3^- uptake became relevant at pH $\geq$ 8.1 (equivalent to CO_2 concentrations $\leq$ 14 µmol L^{-1}), particularly in low pCO_2-acclimated cells. Except for haploid cells measured at pH 8.1, no significant differences in f_{CO_2} were observed between the low and high pCO_2 acclimations (Fig. 2b).

The sensitivity analysis showed that an offset in the input pH of the buffered assay cell suspension (± 0.05 pH units) led to deviations in f_{CO_2} of $\leq$ 0.09 (i.e., 9 percentage points) in "CO_2 users" and $\leq$ 0.02 in "HCO_3^- users" (Fig. 3a). An offset in the input temperature of the assay buffer (± 2 °C) led to a deviation in f_{CO_2} of $\leq$ 0.09 in "CO_2 users" and $\leq$ 0.03 in "HCO_3^- users" (Fig. 3a). An offset in the input pH of the spike (± 0.05 pH units) changed the f_{CO_2} estimates by $\leq$ 0.08 in "CO_2 users" and $\leq$ 0.03 in "HCO_3^- users" (Fig. 3a). Applying an offset in the input temperature of the spike (± 2 °C) caused a deviation in f_{CO_2} by $\leq$ 0.06 in "CO_2 users" and had practically no effect on f_{CO_2} in "HCO_3^- users" ($\leq$ 0.01; Fig. 3a). An offset in the input DIC concentration of the buffer (± 100 µmol kg^{-1}) affected f_{CO_2} by $\leq$ 0.08 in "CO_2 users" and $\leq$ 0.03 in "HCO_3^- users". Regarding the radioactivity of the spike (± 37 kBq), deviations in f_{CO_2} were $\leq$ 0.12 in "CO_2 users" and $\leq$ 0.04 in "HCO_3^- users." Irrespective of CO_2 or HCO_3^- usage, offsets in blank estimations (± 100 dpm) led to deviating f_{CO_2} by $\leq$ 0.27, but only when equilibrium ^{14}C fixation rates were $\leq$ 1 dpm s^{-1} (Fig. 3b). When steady-state ^{14}C incorporation rates were $\geq$ 2 dpm s^{-1} (i.e., average rate in diploid cells) and $\geq$ 4 dpm s^{-1} (i.e., average rate in haploid cells), the deviations in f_{CO_2} due to offsets in the blanks were $\leq$ 0.17 and $\leq$ 0.11, respectively.

Discussion

Acclimation responses

This study corroborates previous findings on the general sensitivity of the diploid life-cycle stage of *E. huxleyi* toward OA (e.g., Feng et al. 2008; Langer et al. 2009; Riebesell et al. 2000). While growth rate was unaffected, OA reduced PIC production and stimulated POC production (Table 3). Consequently, the PIC:POC ratio was strongly decreased under OA, indicating a redirection of C_i fluxes between these two processes. Transcriptomics have previously attributed this redirection to an inhibition of calcification in response to impaired signal-transduction and ion-transport, as well as to stimulation in the production of glycoconjugates and lipids (Rokitta et al. 2012). In our study, also the TPC production increased significantly under OA (Table 3), indicating that not only C_i is allocated differently, but also the overall C_i uptake increases with the increasing pCO_2. Our data further suggest that less energy is required for the C_i acquisition under OA as more POC and TPC could be produced even though the Chl *a* quota

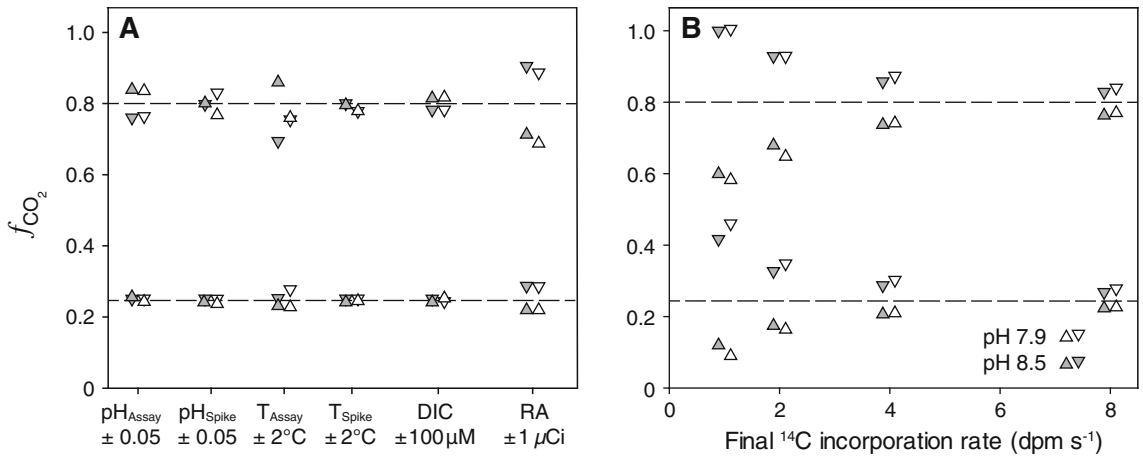

Fig. 3 Sensitivity in f_{CO_2} estimates for "CO_2 users" ($f_{CO_2} = 0.80$) and "HCO_3^- users" ($f_{CO_2} = 0.25$) at low pH (7.9, *in gray*) and high pH (8.5, *in white*) **A** toward negative (*inverted filled triangle*) and positive (*filled triangle*) offsets in the pH, temperature, and DIC concentration of the assay buffer (pH_{Assay}, T_{Assay}, and [DIC]), as well as toward offsets pH, temperature, and radioactivity of the spike (pH_{Spike}, T_{Spike}, and RA), and **B** toward negative (*inverted filled triangle*) and positive (*filled triangle*) offsets in blank measurements (±100 dpm) in dependence of the final ^{14}C incorporation rates. Sensitivity was assessed based on theoretical curves with constraints of a $[DIC]_{Assay} = 2{,}300$ µM, $T_{Assay} = 15$ °C, $T_{Spike} = 23$ °C, and $RA_{Spike} = 37$ kBq. *Dashed lines* indicate f_{CO_2} values as expected for optimal experimental conditions

remained unaffected by the pCO_2 treatment (Table 3). Improved energy-use efficiencies under OA have previously been proposed for the diploid life-cycle stage of *E. huxleyi* (Rokitta and Rost 2012).

In strong contrast to the diploid strain, the haploid life-cycle stage of *E. huxleyi* was insensitive toward OA with respect to growth rate and elemental composition (Table 3). The ability of the haploid cells to maintain homeostasis under OA has also been observed by Rokitta and Rost (2012). Even though the haploid cells appeared non-responsive toward OA on the phenomenological level (i.e., growth, elemental composition), transcriptomics have revealed significant changes at the subcellular level, such as an upregulation of catabolic pathways under OA (Rokitta et al. 2012). Based on the comparison of the life-cycle stages, Rokitta and co-workers concluded that the OA sensitivity in diploid cells originates from calcification, differences in C_i acquisition or both.

A number of studies have shown that *E. huxleyi* has moderately high C_i affinities and uses HCO_3^- as the primary C_i source (e.g., Herfort et al. 2002; Rokitta and Rost 2012; Rost et al. 2006b; Stojkovic et al. 2013), irrespective of the degree of calcification (Trimborn et al. 2007; Rokitta and Rost 2012). These characteristics would suggest *E. huxleyi* to be rather insensitive toward OA and the associated rise in CO_2 concentration, contrary to most results obtained for the diplont. As discussed below, this apparent discrepancy could originate from differences in conditions applied during short-term physiological measurements and those conditions cells experience in the long-term acclimation.

Modes of C_i acquisition

Our results demonstrate that the C_i source of both life-cycle stages of *E. huxleyi* is significantly influenced by the pH of the assay medium and the resulting carbonate chemistry (Fig. 2). With increasing pH in assay buffers, cells progressively changed from predominant CO_2 usage at lower pH values (≤ 8.1) to significant HCO_3^- contribution at higher pH (≥ 8.3). Surprisingly, this change occurred irrespectively of the pCO_2 conditions in the acclimation. To our knowledge, such a strong short-term pH-dependence in C_i acquisition has not been previously reported, which is most likely due to the fact that assays are typically performed under standardized pH values. Measuring physiological responses under one reference condition have the advantage that consequences of different acclimations can readily be compared in terms of altered capacities of certain processes, e.g., enzyme activities or transport rates. However, determination of the C_i source at one standard pH appears to impose a methodological bias, and our results, therefore, bear direct relevance to the interpretation of previous laboratory observations.

In view of the short-term pH effect on C_i acquisition, the contribution of HCO_3^- as a photosynthetic C_i source in *E. huxleyi* may have possibly been overestimated in previous studies. This overestimation is likely to be the most significant in those studies when ^{14}C disequilibrium assays were conducted at pH 8.5 (e.g., Rokitta and Rost 2012; Rost et al. 2007). By looking at the C_i source determined at an assay pH mimicking the acclimation condition, we can now re-evaluate and in fact explain the responses of

E. huxleyi toward elevated pCO_2. When assessing f_{CO_2} using assay buffers of pH 7.9 and 8.1 (equivalent to the acclimation pH of high and low pCO_2 treatments), we observed predominant CO_2 uptake under both conditions (Fig. 2). Being "CO_2 user", cells were thus able to directly benefit from changes in the CO_2 concentrations in our acclimations ($\sim$15 µmol kg^{-1} at 380 µatm and $\sim$38 µmol kg^{-1} at 950 µatm). For a "HCO_3^- user", however, it would be difficult to argue for a beneficial OA-effect as HCO_3^- concentrations do not differ much between treatments ($\sim$1,930 µmol kg^{-1} at 380 µatm and $\sim$2,130 µmol kg^{-1} at 950 µatm). Our results thus suggest that biomass production in diploid cells not only profits from the declined calcification at high pCO_2, as suggested by Rokitta and Rost (2012) but also from the higher CO_2 supply under OA. As CO_2 usage is considered to be less costly than HCO_3^- uptake (Raven 1990), this could also explain the higher energy-use efficiency observed for *E. huxleyi* (Rokitta and Rost 2012).

Although the haploid life-cycle stage of *E. huxleyi* exhibited a pH-dependent C_i uptake behavior that was similar to the diploid (Fig. 2), the haploid cells did not show any CO_2-dependent stimulation in biomass production (Table 3). This could partly be related to the fact that the biomass production cannot profit from a down-scaling of calcification, simply because this process is absent in the haploid life-cycle stage. The lack of significantly stimulated biomass buildup under OA could also be attributed to the concomitant upregulation of catabolic pathways, such as higher lipid consumption, which is a specific feature of the haploid cells (Rokitta et al. 2012). After all, the similar C_i uptake behavior of both life-cycle stages confirms that photosynthetic HCO_3^- usage is not tied to calcification (Herfort et al. 2004; Trimborn et al. 2007; Bach et al. 2013) and that the preference for CO_2 or HCO_3^- is predominantly controlled by carbonate chemistry.

Our findings clearly demonstrate that the acclimation history, in both life-cycle stages, has little or no effect on the C_i usage of the cells (Fig. 2). In other words, the instantaneous effect of the assay conditions dominates over acclimation effects. We cannot preclude, however, that cells acclimated to higher pH values, where CO_2 supply becomes limiting, may increase their capacity for HCO_3^- uptake and acclimations effects would then be evident. Notwithstanding the potential for some acclimation effects, the extent to which short-term pH and/or CO_2 levels in the assay medium directly control cellular C_i usage is striking. This implies that even though *E. huxleyi* did not use significant amounts of HCO_3^- for photosynthesis, it must constitutively express a HCO_3^- transporter in all acclimations. Without the presence of a functional HCO_3^- transport system we could otherwise not explain the capacity for significant HCO_3^- uptake under short-term exposure to high pH (even in high pCO_2-acclimated cells).

In the diploid life-cycle stage, HCO_3^- transporter may be constitutively expressed to fuel calcification, as HCO_3^- was identified as the main C_i source for this process (Paasche 1964; Rost et al. 2002; Sikes et al. 1980). If CO_2 supply for photosynthesis becomes limiting, HCO_3^- transport could then also fuel photosynthesis. In the haploid cells, which do not calcify, we nonetheless observed the same capacity for HCO_3^- uptake, which suggests that HCO_3^- uptake capacity represents a fundamental component of the CCM of both life-cycle stages of *E. huxleyi*. Whether levels of protons or CO_2 concentrations are the main trigger for the shift between CO_2 and HCO_3^- uptake remains unclear, even though there is strong evidence that CO_2 supply is the main driver for the responses in photosynthesis (Bach et al. 2011).

Sensitivity analyses

In our sensitivity study, the applied offsets in pH (± 0.05 pH units), temperature (± 2 °C), DIC of the assay buffer (± 100 µM), and spike radioactivity (± 37 kBq) were larger than typical measurement errors to represent "worst-case scenarios". None of these offsets caused f_{CO_2} estimates to deviate by more 0.12 in any of the pH treatments (Fig. 3a). When adequate efforts are taken to control these parameters (e.g., using reference buffers, thermostats), methodological uncertainties are thus negligible. DIC concentrations and radioactivity, however, are often not measured and in view of the potential drift over time, offsets can easily exceed typical measurement errors and lead to severe deviations in f_{CO_2}. For instance, $^{14}CO_2$ out-gassing causes the spike solution to progressively lose radioactivity. This loss of ^{14}C can easily be > 20 % over the course of weeks or months, despite the high pH values of the stock solution and small headspace in the storage vial (Gattuso et al. 2010).

The average final ^{14}C fixation rates, which depend on the biomass and radioactivity used, were 2.1 ± 0.8 dpm s^{-1} in the runs with diploid and 6.6 ± 2.2 dpm s^{-1} in those with haploid cells (Fig. 3b). In these ranges, offsets in blank values (± 100 dpm) can lead to biases in the estimated f_{CO_2} by up to 0.20 (Fig. 3b). This strong sensitivity highlights the need to thoroughly determine blank values, but also to work with sufficiently high biomass and/or radioactivity to maximize ^{14}C incorporation rates. When working with dense cell suspensions, however, self-shading or significant drawdown of DIC during the assay might bias results. Higher label addition generally increases the resolution of the assay and lowers the consequences of offsets in the blank value. It should be noted, however, that high concentrations of ^{14}C in

spike solutions can affect not only the isotopic but also the chemical conditions in the cuvette (e.g., pH and DIC).

Overall, our sensitivity study revealed that the ^{14}C disequilibrium method is a straightforward and robust assay, which is very useful for resolving the C_i source of phytoplankton over a range of different pH values. It is important to realize, however, the pH of assay buffers has the potential to significantly affect the C_i uptake behavior of cells.

Conclusions

Our data clearly demonstrate that both life-cycle stages of *E. huxleyi* predominantly use CO_2 as C_i source for photosynthesis under typical present-day and future CO_2 levels, but constitutively express HCO_3^- transporters allowing them to directly use HCO_3^- when CO_2 becomes limiting. Under bloom conditions, where pH values can easily increase to 8.5 or higher, cells might, therefore, be able to maintain efficient C_i acquisition. Future research needs to investigate whether and how the assay pH governs the mode of C_i acquisition also in other coccolithophores species or phytoplankton taxa and how this may alter the energy budget of cells. Results from previous studies may need re-consideration in the light of our data showing strong short-term pH effects on C_i uptake of phytoplankton.

Acknowledgments We thank Silke Thoms and Lena Holtz for the discussion of our data and their constructive feedback on this manuscript. This work was supported by the European Community's Seventh Framework Programme/ERC grant agreement #205150, and by an Alexander Von Humboldt fellowship to PDT.

References

Anning T, Nimer N, Merrett M, Brownlee C (1996) Costs and benefits of calcification in coccolithophorids. J Mar Syst 9:45–56

Bach LT, Riebesell U, Schulz KG (2011) Distinguishing between the effects of ocean acidification and ocean carbonation in the coccolithophore *Emiliania huxleyi*. Limnol Oceanogr 56:2040–2050

Bach LT, Mackinder LCM, Schulz KG, Wheeler G, Schroeder DC, Brownlee C, Riebesell U (2013) Dissecting the impact of CO_2 and pH on the mechanisms of photosynthesis and calcification in the coccolithophore *Emiliania huxleyi*. New Phytol 199:121–134

Badger MR (2003) The roles of carbonic anhydrases in photosynthetic CO_2 concentrating mechanisms. Photosynth Res 77:83–94

Broecker WS, Peng T-H (1982) Tracers in the Sea. EldigioPress, New York

Caldeira K, Wickett ME (2003) Anthropogenic carbon and ocean pH—the coming centuries may see more oceanic acidification than the past 300 million years. Nature 425:365

Cassar N, Laws EA, Bidigare RR, Popp BN (2004) Bicarbonate uptake by Southern Ocean phytoplankton. Glob Biogeochem Cy 18:GB2003. doi:10.1029/2003GB002116

Dickson AG (1981) An exact definition of total alkalinity and a procedure for the estimation of alkalinity and total inorganic carbon from titration data. Deep Sea Res 28A:609–623

Dickson AG (1990) Standard potential of the reaction: $AgCl(s) + ½ H_2(g) = Ag(s) + HCl(aq)$, and the standard acidity constant of the ion HSO_4^- in synthetic seawater from 273.15 to 318.15 K. J Chem Thermodyn 22:113–127

Dickson AG, Millero FJ (1987) A comparison of the equilibrium constants for the dissociation of carbonic acid in seawater media. Deep Sea Res 34:1733–1743

Elzenga JTM, Prins HBA, Stefels J (2000) The role of extracellular carbonic anhydrase activity in inorganic carbon utilization of *Phaeocystis globosa* (Prymnesiophyceae): a comparison with other marine algae using the isotopic disequilibrium technique. Limnol Oceanogr 45:372–380

Espie GS, Colman B (1986) Inorganic carbon uptake during photosynthesis—a theoretical analysis using the isotopic disequilibrium technique. Plant Physiol 80:863–869

Falkowski PG, Barber RT, Smetacek V (1998) Biogeochemical controls and feedbacks on ocean primary production. Science 281:200–206

Feng Y, Warner ME, Zhang Y, Sun J, Fu FX, Rose JM, Hutchins DA (2008) Interactive effects of increased pCO_2, temperature and irradiance on the marine coccolithophore *Emiliania huxleyi* (Prymnesiophyceae). Eur J Phycol 43:87–98

Field CB, Behrenfeld MJ, Randerson JT, Falkowski P (1998) Primary production of the biosphere—integrating terrestrial and oceanic components. Science 281:237–240

Frada MJ, Bidle KD, Probert I, de Vargas C (2012) *In situ* survey of life cycle phases of the coccolithophore *Emiliania huxleyi* (Haptophyta). Environ Microbiol 14(6):1558–1569

Gattuso J-P, Gao K, Lee K, Rost B, Schulz K (2010). Approaches and tools to manipulate the carbonate chemistry, In: Riebesell U, Fabry VJ, Hansson L, Gattuso J-P (eds) Guide for best practices in ocean acidification research and data reporting. European Commission, pp 41–52

Guillard RRL, Ryther JH (1962) Studies of marine planktonic diatoms. Can J Microbiol 8:229–239

Herfort L, Thake B, Roberts J (2002) Acquisition and use of bicarbonate by *Emiliania huxleyi*. New Phytol 156:427–436

Herfort L, Loste E, Meldrum F, Thake B (2004) Structural and physiological effects of calcium and magnesium in *Emiliania huxleyi* (Lohmann) Hay and Mohler. J Struct Biol 148:307–314

Holm-Hansen O, Riemann B (1978) Chlorophyll a determination: improvements in methodology. Oikos 30:438–447

Hoppe CJM, Langer G, Rost B (2011) *Emiliania huxleyi* shows identical responses to elevated pCO_2 in TA and DIC manipulations. J Exp Mar Biol Ecol 406:54–62

Hoppe CJM, Langer G, Rokitta SD, Wolf-Gladrow DA, Rost B (2012) Implications of observed inconsistencies in carbonate chemistry measurements for ocean acidification studies. Biogeosciences 9:2401–2405

Johnson KS (1982) Carbon dioxide hydration and dehydration kinetics in seawater. Limnol Oceanogr 27:849–855

Langer G, Nehrke G, Probert I, Ly J, Ziveri P (2009) Strain-specific responses of *Emiliania huxleyi* to changing seawater carbonate chemistry. Biogeosciences 6:2637–2646

Mackinder L, Wheeler G, Schroeder D, Riebesell U, Brownlee C (2010) Molecular mechanisms underlying calcification in coccolithophores. Geomicrobiol J 27:585–595

Martin CL, Tortell PD (2006) Bicarbonate transport and extracellular carbonate anhydrase in Bering Sea phytoplankton assemblages:

results from isotopic disequilibrium experiments. Limnol Oceanogr 51:2111–2121

Mehrbach C, Culberson CH, Hawley JE, Pytkowicz RM (1973) Measurement of the apparent dissociation constants of carbonic acid in seawater at atmospheric pressure. Limnol Oceanogr 18:897–907

Millero FJ, Roy RN (1997) A chemical equilibrium model for the carbonate system in natural waters. Croat Chem Acta 70:1–38

Paasche E (1964) A tracer study of the inorganic carbon uptake during coccolith formation and photosynthesis in the coccolithophorid *Coccolithus huxleyi*. Physiol Plant 18:138–145

Paasche E (2002) A review of the coccolithophorid *Emiliania huxleyi* (Prymnesiophyceae), with particular reference to growth, coccolith formation, and calcification-photosynthesis interactions. Phycologia 40:503–529

Pierrot D, Lewis E, Wallace D (2006) MS Excel program developed for CO_2 system calculations. ORNL/CDIAC-105 Carbon Dioxide Information Analysis Center, Oak Ridge National Laboratory, U.S. Department of Energy, Oak Ridge

Raven JA (1990) Sensing pH? Plant Cell Environ 13:721–729

Raven JA (2006) Sensing inorganic carbon: CO_2 and HCO_3^-. Biochem J 396:e5–e7. doi:10.1042/BJ20060574

Raven JA, Crawfurd K (2012) Environmental controls on coccolithophore calcification. Mar Ecol Prog Ser 470:137–166

Read BA, Kegel J, Klute MJ, Kuo A, Lefebvre SC, Maumus F, Mayer C, Miller J, Monier A, Salamov A et al (2013) Pan genome of the phytoplankton *Emiliania* underpins its global distribution. Nature 499:209–213

Reinfelder JR (2011) Carbon concentrating mechanisms in eukaryotic marine phytoplankton. Annu Rev Mar Sci 3:291–315

Riebesell U, Zondervan I, Rost B, Tortell PD, Zeebe E, Morel FMM (2000) Reduced calcification in marine plankton in response to increased atmospheric CO_2. Nature 407:364–367

Rokitta SD, Rost B (2012) Effects of CO_2 and their modulation by light in the life-cycle stages of the coccolithophore *Emiliania huxleyi*. Limnol Oceanogr 57(2):607–618

Rokitta SD, De Nooijer LJ, Trimborn S, De Vargas C, Rost B, John U (2011) Transcriptome analyses reveal differential gene expression patterns between lifecycle stages of *Emiliania huxleyi* (Haptophyta) and reflect specialization to different ecological niches. J Phycol 47:829–838

Rokitta SD, John U, Rost B (2012) Ocean acidification affects redox-balance and ion-homeostasis in the life-cycle stages of *Emiliania huxleyi*. PLoS One 7(12):e52212. doi:10.1371/journal.pone.0052212

Rost B, Zondervan I, Riebesell U (2002) Light-dependent carbon isotope fractionation in the coccolithophorid *Emiliania huxleyi*. Limnol Oceanogr 47:120–128

Rost B, Riebesell U, Burkhardt S, Sültemeyer D (2003) Carbon acquisition of bloom-forming marine phytoplankton. Limnol Oceanogr 48:55–67

Rost B, Richter K-U, Riebesell U, Hansen PJ (2006a) Inorganic carbon acquisition in red tide dinoflagellates. Plant Cell Environ 29:810–822

Rost B, Riebesell U, Sültemeyer D (2006b) Carbon acquisition of marine phytoplankton: effect of photoperiod length. Limnol Oceanogr 51:12–20

Rost B, Kranz SA, Richter KU, Tortell PD (2007) Isotope disequilibrium and mass spectrometric studies of inorganic carbon acquisition by phytoplankton. Limnol Oceanogr Methods 5:328–337

Sikes CS, Roer RD, Wilbur KM (1980) Photosynthesis and coccolith formation: inorganic carbon sources and net inorganic reaction of deposition. Limnol Oceanogr 25:248–261

Stojkovic S, Beardall J, Matear R (2013) CO_2-concentrating mechanisms in three southern hemisphere strains of *Emiliania huxleyi*. J Phycol 49:670–679

Stoll MHC, Bakker K, Nobbe GH, Haese AR (2001) Continuous-flow analysis of dissolved inorganic carbon content in seawater. Anal Chem 73:4111–4116

Suffrian K, Schulz KG, Gutowska MA, Riebesell U, Bleich M (2011) Cellular pH measurements in *Emiliania huxleyi* reveal pronounced membrane proton permeability. New Phytol 190:595–608

Taylor AR, Chrachi A, Wheeler G, Goddard H, Brownlee C (2011) A voltage-gated H^+ channel underlying pH homeostasis in calcifying coccolithophores. PLoS Biol 9(6):14–16

Tortell PD, Morel FMM (2002) Sources of inorganic carbon for phytoplankton in the eastern Subtropical and Equatorial Pacific Ocean. Limnol Oceanogr 47:1012–1022

Tortell PD, Payne CD, Li Y, Trimborn S, Rost B, Smith WO, Riesselman C, Dunbar R, Sedwick P, DiTullio G (2008) The CO_2 response of Southern Ocean phytoplankton. Geophys Res Lett 35:L04605

Trimborn S, Langer G, Rost B (2007) Effect of varying calcium concentrations and light intensities on calcification and photosynthesis in *Emiliania huxleyi*. Limnol Oceanogr 52:2285–2293

Westbroek P, Brown CW, Van Bleijswijk J, Brownlee C, Brummer GJ, Conte M, Egge J, Fernandez E, Jordan R, Knappertsbusch M, Stefels J, Veldhuis M, Van Der Wal P, Young J (1993) A model system approach to biological climate forcing—the example of *Emiliania huxleyi*. Glob Planet Change 8:27–46

Wolf-Gladrow DA, Riebesell U, Burkhardt S, Bijma J (1999) Direct effects of CO_2 concentration on growth and isotopic composition of marine plankton. Tellus 51:461–476

Zeebe RE, Wolf-Gladrow DA (2007) CO_2 in seawater: equilibrium, kinetics, isotopes. Elsevier Science B.V, Amsterdam